

Research Article

Wearable Antennas for Remote Health Care Monitoring Systems

Laura Corchia, Giuseppina Monti, Egidio De Benedetto, and Luciano Tarricone

Department of Engineering for Innovation, University of Salento, 73100 Lecce, Italy

Correspondence should be addressed to Giuseppina Monti; giuseppina.monti@unisalento.it

Received 17 July 2017; Revised 12 September 2017; Accepted 1 November 2017; Published 17 December 2017

Academic Editor: Xianming Qing

Copyright © 2017 Laura Corchia et al. This is an open access article distributed under the Creative Commons Attribution License, which permits unrestricted use, distribution, and reproduction in any medium, provided the original work is properly cited.

Remote monitoring of the elderly in telehealth applications requires that the monitoring must not affect the elderly's regular habits. To ensure this requirement, the components (i.e., sensor and antenna) necessary to carry out such monitoring should blend in with the elderly's daily routine. To this end, an effective strategy relies on employing wearable antennas that can be fully integrated with clothes and that can be used for remotely transmitting/receiving the sensor data. Starting from these considerations, in this work, two different methods for wearable antenna fabrication are described in detail: the first resorts to the combined use of nonwoven conductive fabrics and of a cutting plotter for shaping the fabric, whereas the second considered fabrication method resorts to the embroidery of conductive threads. To demonstrate the suitability of the considered fabrication techniques and to highlight their pros and cons, numerical and experimental results related to different wearable antennas are also reported and commented on. Results demonstrate that the presented fabrication techniques and strategies are very flexible and can be used to obtain low-cost wearable antennas with performance tailored for the specific application at hand.

1. Introduction

Health care is an inalienable human right and, as such, it should not be considered a privilege for the few. Nevertheless, budget cuts and spending reviews are seriously affecting public services in many sectors, including health care. In this scenario, the elderly population is often the category that is affected the most by this situation; in fact, hospitals are often unwilling to spend their budget on services for senior citizens. On the other hand, the increase of life expectancy, along with the elderly's undeniable right to live ageing as a positive experience, motivates the need to identify innovative and low-cost technological solutions that could make health care provision more cost-effective and efficient.

In this regard, telemedicine is regarded as one of the key strategies for a substantial reduction of the social costs related to health care, while still providing the necessary support to the elderly and guaranteeing a good quality of life [1]. Wireless technology is a key ally for remote health monitoring [2–10]. In fact, the combination of noninvasive wearable sensors and of information technologies can allow the elderly

to receive the needed assistance, while continuing to live in their own homes, rather than in impersonal and expensive nursing homes [1].

Accordingly, at the state of the art, several solutions are available dedicated to activity recognition to extract information on habitat behavior [2–6] and to detect possible anomalies in health parameters [7–10].

Among these, in [2], a system (consisting of a microwave radar sensor and a wirelessly connected base station for data processing) for remote fall detection in an indoor environment was presented.

Furthermore, in [9], a suite of home care sensor network system was proposed. It consists of biosensors placed on the body of the patient which transmit measured signals to the remote wireless monitor for acquiring the observed human physiological signals. The monitoring platform was implemented by exploiting the ZigBee and the GSM technology.

Finally, in [10], a sensing textile platform was presented. In this wearable monitoring system, sensors are knitted on the clothes, thus reducing the burden to the patient and guaranteeing a better sensitivity with respect to printed sensors.

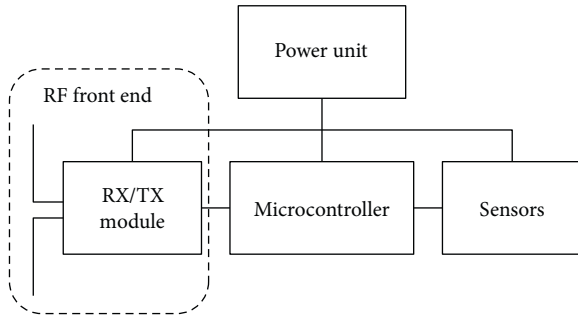


FIGURE 1: General diagram of a wireless monitoring system.

The general architecture of a wireless health care monitoring system is shown in Figure 1. Four major blocks can be identified:

- (i) The RF (radio frequency) front end, which comprises an antenna and an RX/TX (receiving/transmitting) module for receiving/transmitting data from/to the data monitoring unit
- (ii) A microcontroller for processing the data received from the sensors and sends them to block (i)
- (iii) The sensor
- (iv) The power supply unit necessary for operating all the previous blocks

For an effective use of wearable wireless systems, all these four electronic blocks should be integrated into clothes or wearable accessories [10]. Hence, the use of nonconventional fabrication techniques and materials combined with customized design strategies is required.

In this regard, the present paper focuses on fabrication techniques and materials which make the integration of the wireless monitoring platforms into garments easier. In particular, the present work addresses the fabrication of wearable antennas that can be fully integrated with clothes and that can be used for remotely transmitting/receiving the sensor data.

The paper is structured as follows. In Section 2, the general requirements that should be guaranteed by wearable systems dedicated to the elderly's monitoring are discussed. Based on these requirements, in Section 3, two different fabrication techniques are investigated, namely, the use of nonwoven conductive fabrics in combination with a cutting plotter and the embroidery of conductive threads. Successively, Section 4 and Section 5 report the details on the design, fabrication, and characterization of different antenna prototypes using nonwoven conductive fabrics (NWCFs) or conductive threads, respectively. The reported numerical and experimental results demonstrate that the proposed fabrication techniques and strategies are very flexible and can allow obtaining low-cost wearable antennas with performance tailored according to the specific application requirements. Also, through an overview of different wearable antenna prototypes, it is shown that by selecting an appropriate fabrication technique, the antenna and the other blocks of

a wireless health care monitoring system (see Figure 1) can be successfully integrated with clothes. Finally, in Section 6, conclusions are drawn.

2. General Requirements of Wearable Systems for Remote Health Care Monitoring

Before proceeding with the description of the investigated fabrication techniques, it is important to discuss some specific requirements that must be possessed by the wearable antennas to be effectively used for the intended monitoring purposes. As a matter of fact, these requirements motivate the choice of the most suitable technological solutions.

First of all, wearable devices must be useful, comfortable, noninvasive, and unobtrusive to the users. This is particularly true for people who are affected by an illness such as the Alzheimer's disease; in this case, in fact, the ageing condition is usually aggravated by problems related to memory loss. It is not uncommon that people who suffer from Alzheimer's disease leave their homes without reason and start wandering around; in such cases, while they may probably forget their mobile phones or their identification documents, it is less likely that they do not wear their clothes, which are an inherent part of a person's everyday routine. Hence, wearable electronics embedded in clothes become the ideal means for implementing on one hand ubiquitous and continuous health monitoring [8] and on the other hand a tracking system which allows to locate the wandering person. By embedding it in the clothes, the components necessary for remotely monitoring the person and the use of the monitoring system would become an automatic action as getting dressed.

To this purpose, textile materials could be exploited for both the conductive parts and the substrate. Additionally, the conductive parts should be fabricated with materials that allow tin soldering of the necessary electronics (electronic chips and, in general, surface mounted components).

Other important requirements for wearable systems are related to the time and cost of the manufacturing process. In particular, in view of a large-scale production and cost containment, cost-effective and industrially scalable manufacturing techniques should be preferred.

On the basis of these considerations, in the following section, two fabrication techniques and materials that can satisfy all the main requirements of a wearable monitoring system and which allow the fabrication of highly embeddable antennas are discussed in detail.

3. Wearable Antenna Fabrication Techniques

Several textile antennas have been proposed in the literature [11–31]. One of the major differences among them relates to the materials employed for implementing the conductive parts. These materials can be roughly grouped into four main categories:

- (a) NWCFs [11, 12]
- (b) Conductive threads [13–16]
- (c) Electro-textiles [17–25]

TABLE 1: Comparison between conductive materials used for fabricating wearable antennas.

	NWCFs	Conductive material		
		Threads	Electro-textiles	Inks
Conductivity	High	Low	High	Low
Spatial resolution	High	High	Low	Low
Fraying	No	No	Yes	No
Washability	Yes	Yes	Yes	Yes
Cost	Low	High	High	Low
Ref.	This work	[13]	[24, 25]	[26–29]

(d) Conductive inks [26–31]

Generally, materials that fall into the NWCF and conductive thread categories allow to obtain better spatial resolution and better performance in terms of integration of the antenna with the clothes/surface mounted components (see Table 1). In the following, two fabrication techniques that employ these materials are presented and discussed.

3.1. Nonwoven Conductive Fabrics (NWCFs) and Cutting Plotter. NWCFs are generally made of metal or polymer-coated artificial and synthetic fibers also used for fabricating the electro-textiles. However, while the electro-textiles are the results of weaving, NWCFs are fabric-like materials made from long conductive fibers casually arranged and bonded together by chemical or mechanical processes. Hence, NWCFs guarantee properties similar to those of traditional electro-textiles in terms of flexibility, mechanical resistance, washability, conductivity, and so on, exhibiting no fraying problems (see Table 1). This feature is essential for obtaining shapes with small and complicated geometries. As shown in Section 4, it also allows to cut adhesive foils of nonwoven conductive fabrics simply by means of a cutting plotter commonly used in the graphics industry for shaping vinyl sheets. This results in a cost-effective and time-saving manufacturing process.

Another advantage of NWCFs is that these materials can be soldered. This property allows to integrate the wearable antennas with sensors and with electronic chips in general.

As a result of these numerous advantages, NWCFs have been rapidly replacing traditional electro-textiles.

A low-cost antenna manufacturing technique exploiting a cutting plotter was originally proposed in [32] for fabricating UHF RFID tags made out of adhesive copper tape. The use of NWCFs in combination with a cutting plotter for fabricating wearable antennas was demonstrated for the first time in [33]. The proposed fabrication technique consists of five major steps:

- (1) Numerical modeling of the antenna and full-wave simulations to identify the antenna geometry and dimensions that could satisfy the application requirements
- (2) Shaping the antenna by cutting the adhesive conductive fabric through a cutting plotter

- (3) Sticking an adhesive vinyl foil on the conductive fabric and removing the backing material

- (4) Sticking the conductive fabric on the textile substrate

- (5) Removing manually the adhesive vinyl foils and the extra conductive fabric

Clearly, the cutting plotter parameters must be appropriately set in order to maximize the accuracy of the cutting and also in order to avoid cutting the backing material (whose integrity is crucial for carrying out step number 3 and number 4; in fact, it should be removed right before sticking the conductive fabric on the textile substrate).

The resolution that can be achieved through this fabrication technique is determined both by the mechanical characteristics of the conductive material (in particular, by its frailty) and by the cutting plotter resolution (many commercial cutting plotters easily guarantee resolution in the order of $250\ \mu\text{m}$). In practical applications, however, it is recommended to avoid fabricating an antenna containing elements with dimensions comparable to the resolution of the used plotter [32]. Also, geometries with excessively small dimensions could make it much harder to accurately carry out the aforementioned step number 5.

In the experience of the authors, geometries with gaps and lines narrower than $500\ \mu\text{m}$ and $1\ \text{mm}$, respectively, should be avoided.

3.2. Hand Embroidered Antennas. One of the major advantages of embroidered antennas is that the embroidery becomes one with the textile substrate. This means that, in the final product, the embroidery and the textile substrate are intertwined as a seamless block (as opposed to the antenna being just “attached” to the clothes when other fabrication techniques are used [11, 12, 17–25]). As a result, embroidered antennas are also flexible, and they are not affected by everyday use of the piece of clothing (e.g., wearing, washing [16], and ironing) (see Table 1).

Antennas can be embroidered by hand. However, by using a CAD embroidery machine, it is possible to speed up the manufacturing process and to fabricate antennas with very complex geometry, such as logos, letters, or drawing in general [13].

A decided disadvantage, however, relates to the design phase of these antennas. In fact, an accurate numerical modeling of the antenna embroidery demands a considerable computational effort. For this reason, when modeling the embroidered antenna in electromagnetic simulation software, the designer should consider whether to use a simplified numerical model at the expense of the accuracy of simulation results [34].

4. NWCF-Based Wearable Antennas

To test the performance of the manufacturing technique based on the combined use of NWCFs and the cutting plotter, an antenna mimicking the Levi’s logo was designed and fabricated using a NWCF produced by Soliani EMC (model: RS CU C4) with surface resistivity approximately equal to

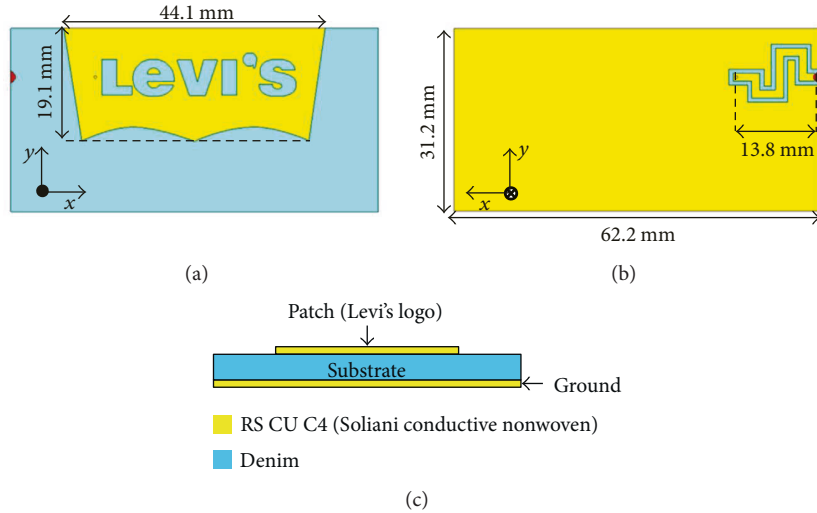


FIGURE 2: Levi's logo antenna design geometry: (a) front view; (b) back view; and (c) side view.

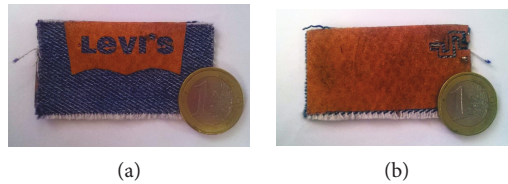


FIGURE 3: Prototype of the proposed NCWF-based logo antenna: (a) front view and (b) back view.

0.03 Ω /sq and thickness of 0.15 mm [35]. A layer of denim, with relative dielectric permittivity $\epsilon_r = 1.67$ and thickness of 0.5 mm, was used as a substrate.

Generally, for wearable applications, an antenna with a patch-like radiation should be preferred; in fact, this configuration would allow not only to limit electromagnetic compatibility issues but also to achieve a platform-tolerant performance, thus enabling the operation in close proximity to the human body. In order to satisfy these requirements, the microstrip technology was chosen.

The Levi's logo was recreated by appropriately shaping the edges of the patch and by using slots to reproduce the writing. To match the antenna impedance to 50 Ω , a coplanar feed line slotted on the ground and shorted to the radiating element by means of a via hole was used.

In order to obtain the desired behavior, the dimensions of the antenna geometry were optimized by means of full-wave simulations carried out through the commercial software CST Microwave Studio (CST MWS) [36]. The optimized dimensions of the antenna are reported in Figure 2, which shows a sketch of the antenna geometry. As for the size of the coplanar feed line and via hole, the width of the line is equal to 1.35 mm, the gap between the feed line and the ground is equal to 0.7 mm, and the via hole has a diameter of 0.5 mm.

Based on the simulation results, a prototype of the proposed antenna was fabricated by cutting the NWCF through a cutting plotter. Figures 3(a) and 3(b) show the

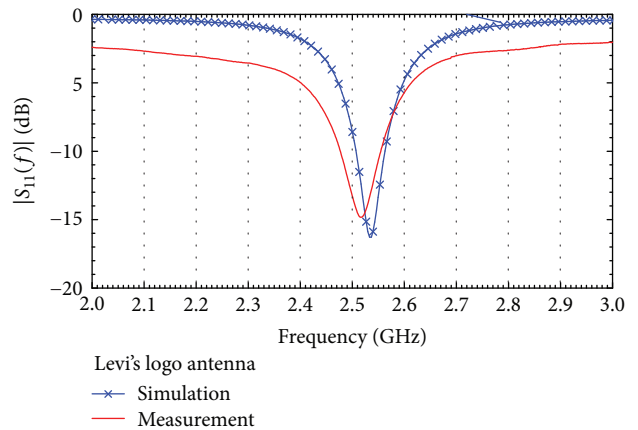


FIGURE 4: Comparison between the simulated and the measured reflection scattering parameter, $|S_{11}(f)|$, for Levi's logo antenna.

pictures of the front and the back of the fabricated prototype, respectively.

The performance of the fabricated antenna was characterized through a vector network analyzer (VNA R&S ZVA50). For the measurements, a 50 Ω SMA connector was tin soldered to the antenna, thus allowing the connection to the VNA. Figure 4 shows the comparison between experimental and numerical results obtained for the reflection coefficient, $|S_{11}(f)|$; a good overall agreement can be noticed.

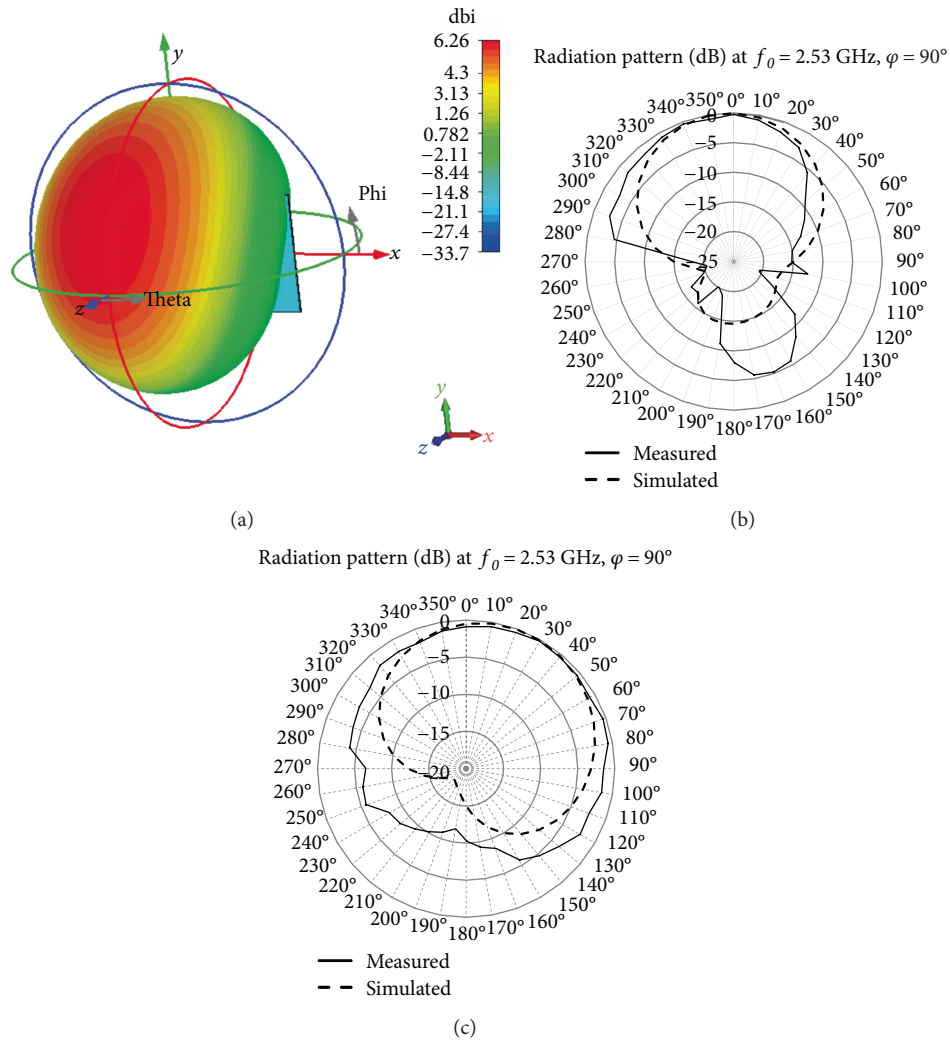


FIGURE 5: Radiation pattern of the proposed logo antenna: (a) simulated 3-D radiation pattern; (b) comparison between numerical data (dashed black curve) and experimental results (continuous black curve) obtained for the x-z plane radiation pattern; and (c) comparison between numerical data (dashed black curve) and experimental results (continuous black curve) obtained for the y-z plane radiation pattern.

As for the radiation properties, the full-wave simulation results obtained through CST MWS are reported and compared with the experimental data in Figure 5. From the numerical data, the direction of maximum irradiation at the central frequency, $f_0 = 2.53$ GHz, is $\phi = 90^\circ$ and $\theta = 22^\circ$, which corresponds to a directivity of 6.26 dBi (see Figure 5(a)). The results shown in Figures 5(b) and 5(c) refer to the planes $\phi = 0^\circ$ and $\phi = 90^\circ$ and confirm the expected radiation pattern of a patch antenna operating in its fundamental TM₁₀₀ mode. Measurements were performed by using a Vector Signal Generator R&S SMBV100A as a source. The distance between the transmitting antenna (a rubber ducky antenna) and the antenna under test (AUT) was set in order to satisfy the far-field region condition. In particular, the most stringent condition between $d \geq 2D^2/\lambda$ ($= 2.72$ cm at 2.53 GHz) and $d \geq 3\lambda$ ($= 35.5$ cm at 2.53 GHz) can be used. Accordingly, measurements were performed by placing the transmitting monopole at a distance of 1.2 m from the AUT. Both the source and the AUT were placed at 1.5 m

from the floor. Finally, the AUT was fixed to a turntable and manually rotated.

The gain measured at $f_0 = 2.53$ GHz in the direction ($\phi = 0^\circ$, $\theta = 90^\circ$) is -5.13 dB, while that obtained from full-wave simulations is -4.83 dB. As for the F/B ratio, the measured values obtained for the planes $\phi = 0^\circ$ and $\phi = 90^\circ$ are 7.8 dB and 10 dB, respectively.

It is worth noting that the results obtained herein and the results reported in [11] for a reconfigurable logo antenna (operating in the GSM and GPS L1 bands) fabricated using a different NWCF on a layer of leather demonstrate that this fabrication technique is suitable to be employed on different kinds of NWCFs. These results also demonstrate that the adhesive-backed NWCFs can be attached on rough textile substrates.

The flexibility of the fabrication technique based on the combined use of self-adhesive NWCFs and a cutting plotter is confirmed by the results reported in Section 4.1 which refer to small and more complex antenna layouts.



FIGURE 6: Wearable antenna prototypes realized by using for the conductive part's adhesive conductive nonwoven fabrics. (a) An antenna which mimics the shape of Giorgio Armani's logo. (b) An antenna which mimics the shape of Lacoste's logo. (c) Wearable resonators having an elliptical loop geometry. (d) Wearable resonators exploiting a complementary split ring resonator geometry. (e) Wearable rectenna. (f) Bow tie-like UHF RFID tag.

4.1. Fabrication of Miniaturized and Complicated Geometries.

As aforementioned, the manufacturing technique based on the use of a cutting plotter can be effectively used for shaping also miniaturized antennas with complicated geometries. For the sake of example, Figure 6(a) shows a picture of a very small antenna (overall dimensions: $25\text{ mm} \times 25\text{ mm}$) designed to work at 1.8 GHz . Also, in this case, the antenna mimicked the logo of a famous fashion brand, namely Giorgio Armani's. In this antenna, in order to achieve a dipole-like radiation pattern, two slits having a width of 1 mm were used to cut the current path on letter A, while two SMD inductors were used for matching the antenna with respect to an input impedance of $50\ \Omega$. As can be seen from Figure 6(a), the $50\ \Omega$ impedance port is inserted between the letters A and G.

The cutting plotter technique and the NWCFs can also be used to fabricate antennas with complicated geometries, such as the one shown in Figure 6(b), which mimics Lacoste's logo. The antenna, which was originally proposed in [37], consists

of a proximity fed planar monopole on a ground plane optimized to work at 1.8 GHz ; the substrate is a 0.5 mm thick layer of jeans. The monopole mimics the crocodile, and the name Lacoste has been subtracted from the ground plane. The overall dimensions are approximately $64.3\text{ mm} \times 51.8\text{ mm}$. The antenna has a relative bandwidth of 20% and a Vivaldi-like radiation pattern with a maximum of the directivity at 1.8 GHz of 4.55 dBi . The parts of the antenna which were more complex to fabricate were the crocodile's squamae and some details of the jaws and of the legs (indicated in the zoom of Figure 6(b)). The achieved results confirm that the proposed fabrication technique allows obtaining good spatial resolution and, in particular, that it can be exploited for fabricating antennas with complex geometries.

Furthermore, Figures 6(c) and 6(d) show the photographs of two wearable resonators proposed for power transfer applications in [38, 39], respectively. These results demonstrate that the proposed manufacturing technique can be exploited for fabricating circular and elliptical loops/geometries.

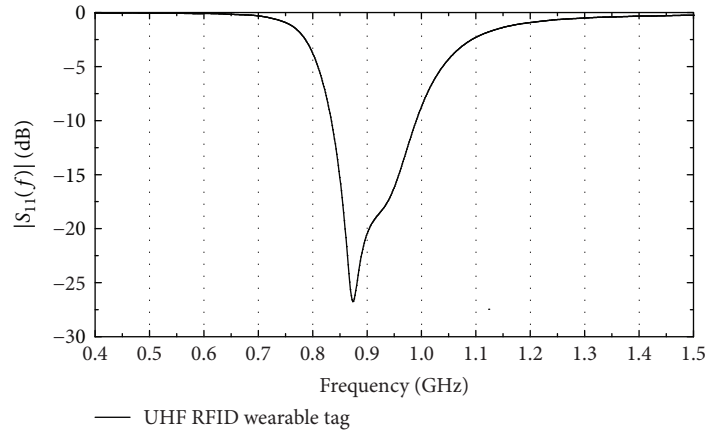


FIGURE 7: Simulated reflection coefficient of the UHF RFID tag reported in Figure 6(f).

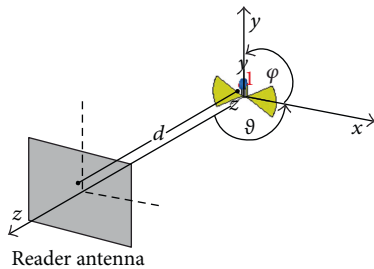


FIGURE 8: Test setup adopted for the characterization of the UHF tag shown in Figure 6(f).

Finally, Figures 6(e) and 6(f) show two prototypes in which the NWCFs were tin soldered, thus allowing the integration of the antenna with electronic parts (see Figure 1). In particular, Figure 6(e) shows the details of the rectenna proposed in [33]. An NWCF was used for implementing all the conductive parts, including the full-wave rectifier exploited for converting the received RF power into DC voltage.

As for the devices shown in Figure 6(f), it is a UHF RFID tag. A bow tie-like geometry [40] was exploited for achieving an operating band covering the European, American, and Japanese bands dedicated to UHF RFID applications [41]. The tag antenna was designed through full-wave simulations performed in CST MWS. The geometry was optimized so as to match the input impedance of the Impinj Monza 3 chip [42]. The numerical results reported in Figure 7 confirm a -10 dB bandwidth in the 834–990 MHz frequency range.

A prototype was fabricated on a 1 mm thick layer of pile. Experimental tests were performed in order to evaluate the sensitivity, the radiation pattern, and the read range of the prototype. The experimental setup adopted for the measurements is shown in Figure 8. As a source, an Impinj Speedway R420 reader equipped with a circularly polarized antenna UPA25 was used. The prototype was characterized in the UHF RFID European band, more specifically, at the frequency $f=867.5$ MHz. From measurements, the tag has a sensitivity of -14.3 dBm and a read range of 4.5 m (when the transmitted power is 30 dBm). As for the radiation

Radiation pattern (dB) at $f = 867.5$ GHz, $\varphi = 90^\circ$

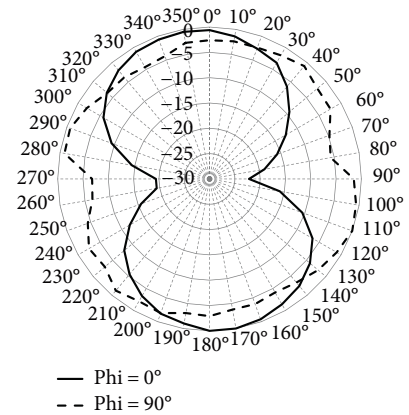


FIGURE 9: Radiation pattern of the UHF RFID tag shown in Figure 6(f), experimental results obtained for the x - z plane radiation pattern (black curve) and for the y - z plane radiation pattern (dashed black curve).

TABLE 2: Dimensions of the antennas shown in Figure 6.

	Overall dimensions (mm)	Minimum dimensions (mm)
Figure 6(a)	25 × 25	1
Figure 6(b)	64.3 × 51.8	0.3
Figure 6(c)	54.7 × 47.6	0.6
Figure 6(d)	57.1 × 55.1	1.4
Figure 6(e)	240 × 190	2
Figure 6(f)	150 × 80	0.5

pattern, Figure 9 shows the experimental results obtained for the $\varphi = 0^\circ$ and for the $\varphi = 90^\circ$ planes (see Figure 8).

The details of the dimensions of the antennas illustrated in Figure 6 are summarized in Table 2.

4.2. *Durability Test.* To test the durability of antennas fabricated using an adhesive-backed NWCF, a washing,

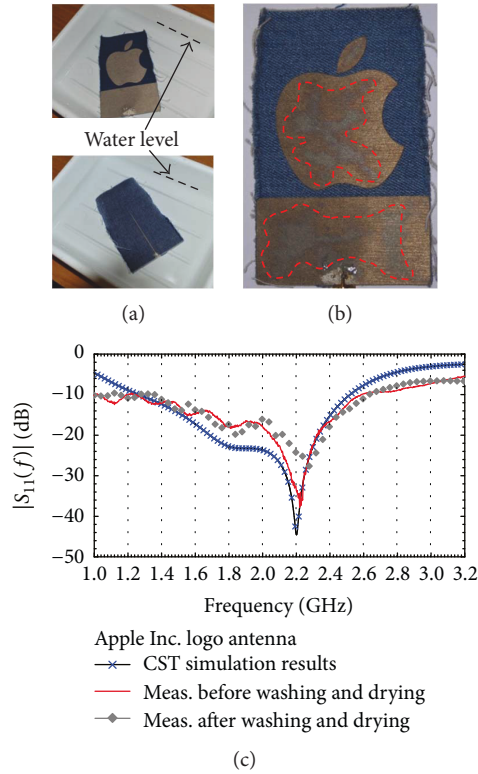


FIGURE 10: (a) Photographs of the antenna immersed in water. (b) Picture of the Apple Inc. logo antenna after the durability test. (c) Comparison between the measured reflection scattering parameter before and after the durability test for the Apple Inc. logo antenna. The simulated reflection scattering parameter is also reported.

drying, and ironing test was performed on the wearable antenna proposed in [12]. The antenna was a proximity-fed planar monopole on a ground plane, wherein the monopole geometry mimicked the logo of the famous Apple Inc. company.

This antenna was fabricated using a jean substrate (relative dielectric permittivity, $\epsilon_r = 1.67$) with a thickness of 0.5 mm. The dimensions of the antenna were 7.6 cm \times 12 cm, while the dimensions of the monopole were optimized so to have a working bandwidth centered at 1.8 GHz. This antenna had a dipole-like radiation pattern with a maximum of the directivity at 1.8 GHz of 3.18 dBi. The relative bandwidth calculated by means of full-wave simulations is of about 68%; in fact, the reflection scattering parameter is lower than -10 dB in the frequency band 1.25–2.55 GHz.

Figure 10(a) shows the Apple Inc. logo antenna immersed in water. Figure 10(b) shows a picture of the antenna after the washing, drying, and ironing; it can be seen that some stains caused by oxidization of the conductive parts are visible (darker area in the picture). To verify if the durability test had compromised the performance of the antenna, the $|S_{11}(f)|$ was measured before and after the test: Figure 10(c) shows the obtained results. It can be seen that, after the test, the antenna still exhibited a performance similar to the one before the durability test. For the sake of completeness, also the results of the $|S_{11}(f)|$ simulated through CST MWS are reported in Figure 10(c).

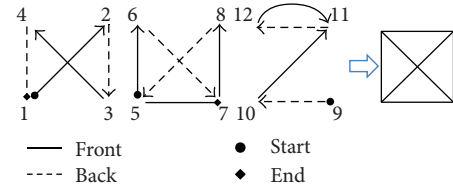


FIGURE 11: Steps for the realization of the conductive path: “back” (black dot line) and “front” (black line) indicate if the path is on the back or on the front side of the fabric.

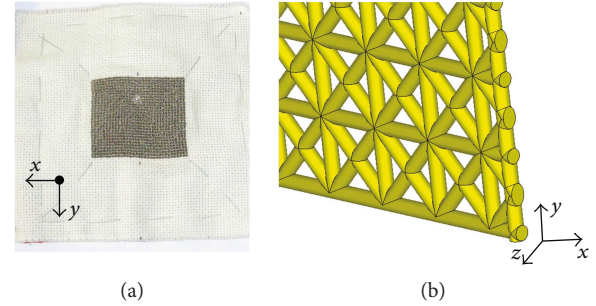


FIGURE 12: (a) Picture of the embroidered patch antenna. (b) Particular of the modified cross-stitch pattern modeled in CST MWS.

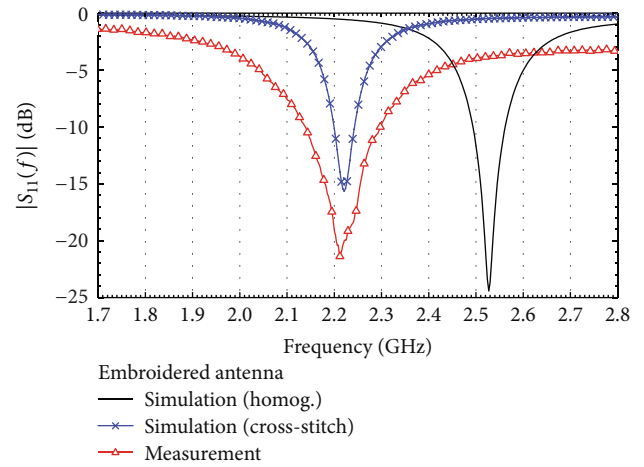


FIGURE 13: Comparison between the simulation results obtained by simulating the patch as a homogeneous layer (black continuous curve) and with a cross-stitch pattern (blue curve with cross markers) for the embroidered patch antenna. The measurement results are also reported (red curve with triangular markers).

It is worth mentioning that a possible strategy to further improve the durability of the antenna could be to use conformal protective coatings [25] or stitching the conductive parts to the substrate by means of nonconductive threads [20].

5. Embroidered Antenna

In this section, the fabrication of an embroidered wearable antenna is described. The conductive sewing thread used for this antenna had a surface resistivity $\leq 0.0025 \Omega/\text{sq}$ and a diameter of 0.2 mm. This thread is suitable to be used with

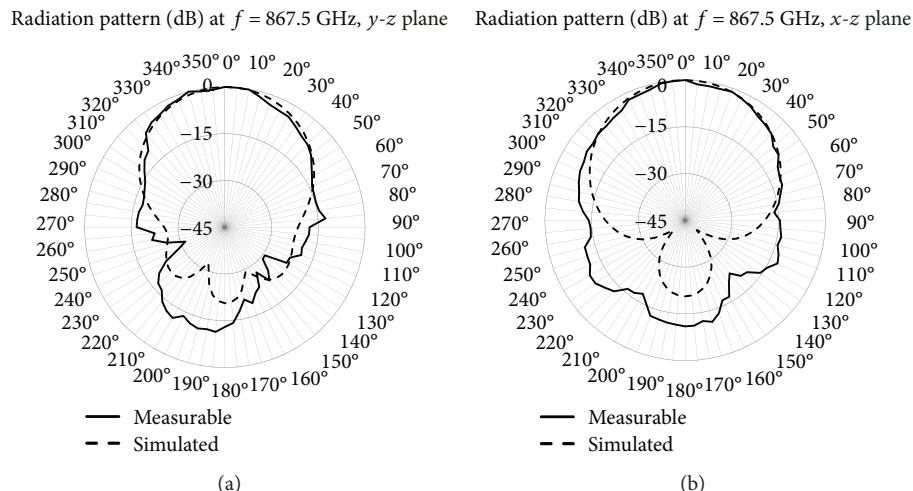


FIGURE 14: Comparison between simulated results and experimental data obtained for the radiation pattern of the embroidered patch antenna: (a) y - z plane and (b) x - z plane.

commercial sewing machines; however, because a CAD-controlled sewing machine was not available, the conductive thread had to be embroidered by hand. For this reason, a simple antenna geometry was chosen, namely, a rectangular patch antenna with a coaxial excitation.

The dimensions of the ground plane are $150 \text{ mm} \times 150 \text{ mm}$, while the dimensions of the patch are $60 \text{ mm} \times 50 \text{ mm}$. The substrate consists of two layers of a pile-like fabric ($\epsilon_r = 1.18$, thickness $h = 2 \text{ mm}$). The conductive thread was embroidered replicating a modified cross-stitch pattern. In Figure 11, the steps necessary to implement the conductive path of a single stitch and the resulting front view of the stitch are illustrated.

Figure 12(a) shows a picture of the fabricated antenna, while Figure 13 shows the reflection scattering parameter of the prototype, $|S_{11}(f)|$, measured through the R&S ZVA50 vector network analyzer. For the sake of comparison, also the $|S_{11}(f)|$ results obtained from two CST MWS simulations are reported: the difference between the reported numerical results is related to the way in which the conductive thread was modeled in the software. In particular, in the first simulation run, the conductive thread was modeled as a homogeneous layer (black curve in Figure 13). This speeded up the computational process but resulted in less accurate results; in fact, the resonance frequency obtained by means of full-wave simulation is higher than the measured one.

Instead, by implementing a more accurate model in CST MWS (by replicating the modified cross-stitch pattern, as shown in Figure 12(b)), the corresponding numerical results (blue curve with cross markers in Figure 13) exhibited a better matching with the measurement results (red curve with triangular markers in Figure 13). In particular, the model illustrated in Figure 12(b) allows to achieve a good agreement between the numerical data and measurements in terms of resonance frequency; however, it can be observed that, even using the model in Figure 12(b), numerical results differ from measurements for the bandwidth and for the value assumed by the $|S_{11}(f)|$. These results suggest the need to use a more accurate model at

the expense of an increase of the computational effort and of the time required for simulations.

As for the radiation properties, experimental measurements were performed by using a software-defined radio (SDR) platform [11, 43, 44]. In particular, the Universal Software Radio Peripheral (USRP) equipped with the XCVR2450 daughterboard [45] and a rubber antenna was used as a signal source. Comparison between simulated and measured results obtained for the radiation pattern at the frequency $f = 2.22 \text{ GHz}$ is shown in Figure 14. As it can be seen, an overall good agreement was achieved.

6. Conclusion

In this work, the fabrication of wearable antennas that could be integrated with sensors for remote monitoring of elderly people was addressed. In particular, two different fabrication methods are described in detail: one resorts to the combined use of adhesive-backed nonwoven conductive fabrics and of a cutting plotter, whereas the other manufacturing technique resorts to the embroidery of conductive threads.

Numerical and experimental results related to the design, fabrication, and characterization of wearable antennas obtained with the considered fabrication techniques were reported and commented on. Results demonstrated that the presented manufacturing methods are very flexible and can be effectively used to obtain a low-cost wearable antenna with performance tailored for the specific application at hand.

Conflicts of Interest

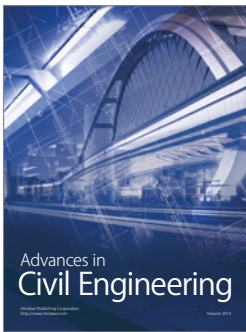
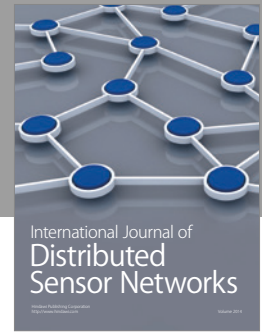
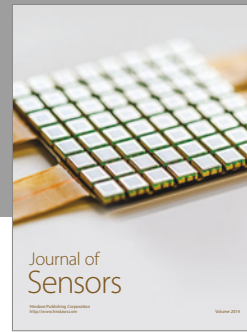
The authors declare that there are no conflicts of interests regarding the publication of this paper.

References

- [1] S. Majumder, T. Mondal, and M. Deen, "Wearable sensors for remote health monitoring," *Sensors*, vol. 17, no. 1, p. 130, 2017.

- [2] C. Garripoli, M. Mercuri, P. Karsmakers et al., "Embedded DSP-based telehealth radar system for remote in-door fall detection," *IEEE Journal of Biomedical and Health Informatics*, vol. 19, no. 1, pp. 92–101, 2015.
- [3] R. Nakamura and H. Hadama, "Target localization using multi-static UWB sensor for indoor monitoring system," in *2017 IEEE Topical Conference on Wireless Sensors and Sensor Networks (WiSNet)*, pp. 37–40, Phoenix, AZ, USA, January 2017.
- [4] F. Viani, M. Martinelli, L. Ioriatti, G. Oliveri, P. Rocca, and A. Massa, "WSN for real-time localization and tracking of elderly people," in *OASIS 1st International Conference*, Florence, Italy, November 2009.
- [5] F. Viani, P. Rocca, G. Oliveri, D. Trincherio, and A. Massa, "Localization, tracking, and imaging of targets in wireless sensor networks: an invited review," *Radio Science*, vol. 46, 2011.
- [6] C. Ungureanu, V. Bui, W. Roosmalen et al., "A wearable monitoring system for nocturnal epileptic seizures," in *2014 8th International Symposium on Medical Information and Communication Technology (ISMICT)*, pp. 1–5, Firenze, Italy, April 2014.
- [7] X. Yu, P. Weller, and K. T. Grattan, "A WSN healthcare monitoring system for elderly people in geriatric facilities," *Studies in Health Technology and Informatics*, pp. 567–571, 2015.
- [8] H. Carvalho, A. P. Catarino, A. Rocha, and O. Postolache, "Health monitoring using textile sensors and electrodes: an overview and integration of technologies," in *2014 IEEE International Symposium on Medical Measurements and Applications (MeMeA)*, pp. 1–6, Lisboa, Portugal, June 2014.
- [9] P. Murali Krishna and K. Padma Priya, "Remote wireless health care monitoring system using ZigBee," *International Journal of Engineering Research and Technology*, vol. 1, pp. 1–4, 2012.
- [10] N. Taccini, G. Loriga, M. Pacelli, and R. Paradiso, "Wearable monitoring system for chronic cardio-respiratory diseases," in *2008 30th Annual International Conference of the IEEE Engineering in Medicine and Biology Society*, pp. 3690–3693, Vancouver, BC, Canada, August 2008.
- [11] G. Monti, L. Corchia, E. De Benedetto, and L. Tarricone, "Wearable logo-antenna for GPS-GSM-based tracking systems," *IET Microwaves, Antennas and Propagation*, vol. 10, no. 12, pp. 1332–1338, 2016.
- [12] G. Monti, L. Corchia, and L. Tarricone, "Logo antenna on textile materials," in *2014 44th European Microwave Conference*, pp. 516–519, Rome, October 2014.
- [13] A. Kiourti, C. Lee, and J. L. Volakis, "Fabrication of textile antennas and circuits with 0.1 mm precision," *IEEE Antennas and Wireless Propagation Letters*, vol. 15, pp. 151–153, 2016.
- [14] J.-S. Roh, Y.-S. Chi, J.-H. Lee, Y. Tak, S. Nam, and T. J. Kang, "Embroidered wearable multiresonant folded dipole antenna for FM reception," *IEEE Antennas and Wireless Propagation Letters*, vol. 9, pp. 803–806, 2010.
- [15] M. A. R. Osman, M. K. Abd Rahim, N. A. Samsuri, H. A. M. Salim, and M. F. Ali, "Embroidered fully textile wearable antenna for medical monitoring applications," *Progress In Electromagnetics Research*, vol. 117, pp. 321–337, 2011.
- [16] M. Toivonen, T. Björninen, L. Sydänheimo, L. Ukkonen, and Y. Rahmat-Samii, "Impact of moisture and washing on the performance of embroidered UHF RFID tags," *IEEE Antennas and Wireless Propagation Letters*, vol. 12, pp. 1590–1593, 2013.
- [17] P. J. Soh, G. A. E. Vandenbosch, S. L. Ooi, and N. H. M. Rais, "Design of a Broadband all-Textile Slotted PIFA," *IEEE Transactions on Antennas and Propagation*, vol. 60, no. 1, pp. 379–384, 2012.
- [18] D. L. Paul, C. Jayatissa, G. S. Hilton, and C. J. Railton, "Conformability of a textile antenna for reception of digital television," in *2010 Loughborough Antennas & Propagation Conference*, pp. 225–228, Loughborough, UK, November 2010.
- [19] D. L. Paul, M. G. Paterson, and G. S. Hilton, "A low-profile textile antenna for reception of digital television and wireless communications," in *2012 IEEE Radio and Wireless Symposium*, pp. 51–54, Santa Clara, CA, USA, January 2012.
- [20] I. Locher, M. Klemm, T. Kirstein, and G. Trster, "Design and characterization of purely textile patch antennas," *IEEE Transactions on Advanced Packaging*, vol. 29, no. 4, pp. 777–788, 2006.
- [21] C. Hertleer, H. Rogier, L. Vallozzi, and L. Van Langenhove, "A textile antenna for off-body communication integrated into protective clothing for firefighters," *IEEE Transactions on Antennas and Propagation*, vol. 57, no. 4, Part 1, pp. 919–925, 2009.
- [22] P. Soh, G. Vandenbosch, S. Ooi, and M. Husna, "Wearable dual-band Sierpinski fractal PIFA using conductive fabric," *Electronics Letters*, vol. 47, no. 6, pp. 365–367, 2011.
- [23] J. Lilja and P. Salonen, "Textile material characterization for SoftWear antennas," in *MILCOM 2009 - 2009 IEEE Military Communications Conference*, pp. 1–7, Boston, MA, USA, 2009.
- [24] W. Thompson, R. Cepeda, G. Hilton, M. Beach, and S. Armour, "An improved antenna mounting for ultra-wideband on-body communications and channel characterization," *IEEE Transactions on Microwave Theory and Techniques*, vol. 59, no. 4, Part 2, pp. 1102–1108, 2011.
- [25] Y. Y. Fu, Y. L. Chan, M. H. Yang et al., "Experimental study on the washing durability of electro-textile UHF RFID tags," *IEEE Antennas and Wireless Propagation Letters*, vol. 14, pp. 466–469, 2015.
- [26] N. Chahat, M. Zhadobov, S. A. Muhammad, L. Le Coq, and R. Sauleau, "60-GHz textile antenna array for body-centric communications," *IEEE Transactions on Antennas and Propagation*, vol. 61, no. 4, pp. 1816–1824, 2013.
- [27] N. Liu, Y. Lu, S. Qiu, and P. Li, "Electromagnetic properties of electro-textiles for wearable antennas applications," *Frontiers of Electrical and Electronic Engineering in China*, vol. 6, no. 4, pp. 563–566, 2011.
- [28] W. G. Whittow, A. Chauraya, J. C. Vardaxoglou et al., "Inkjet-printed microstrip patch antennas realized on textile for wearable applications," *IEEE Antennas and Wireless Propagation Letters*, vol. 13, pp. 71–74, 2014.
- [29] T. Björninen, J. Virkki, L. Sydänheimo, and L. Ukkonen, "Manufacturing of antennas for passive UHF RFID tags by direct write dispensing of copper and silver inks on textiles," in *2015 International Conference on Electromagnetics in Advanced Applications (ICEAA)*, pp. 589–592, Turin, Italy, September 2015.
- [30] Y. Kim, H. Kim, and H. J. Yoo, "Electrical characterization of screen-printed circuits on the fabric," *IEEE Transactions on Advanced Packaging*, vol. 33, no. 1, pp. 196–205, 2010.
- [31] T. Kellomäki, J. Virkki, S. Merilampi, and L. Ukkonen, "Towards washable wearable antennas: a comparison of coating materials for screen-printed textile-based UHF RFID tags,"

- International Journal of Antennas and Propagation*, vol. 2012, Article ID 476570, 11 pages, 2012.
- [32] L. Catarinucci, R. Colella, and L. Tarricone, "Smart prototyping techniques for UHF RFID tags: electromagnetic characterization and comparison with traditional approaches," *Progress In Electromagnetics Research*, vol. 132, pp. 91–91, 2012111, 2012.
- [33] G. Monti, L. Corchia, and L. Tarricone, "UHF wearable rectenna on textile materials," *IEEE Transactions on Antennas and Propagation*, vol. 61, no. 7, pp. 3869–3873, 2013.
- [34] R. Seager, T. Dias, S. Zhang et al., "Effect of the fabrication parameters on the performance of embroidered antennas," *IET Microwaves, Antennas & Propagation*, vol. 7, no. 14, pp. 1174–1181, 2013.
- [35] Soliani EMC, <http://www.solianiemc.com/prodotti/tessuti-con-duttivi-e-schermanti-emi-emc/>.
- [36] CST-Computer Simulation Technology, 2016, <http://www.cst.com>.
- [37] G. Monti, L. Corchia, and L. Tarricone, "Textile logo antennas," in *Proceedings of 2014 Mediterranean Microwave Symposium (MMS2014)*, pp. 1–5, Marrakech, Morocco, December 2014.
- [38] G. Monti, L. Corchia, and L. Tarricone, "A wearable wireless energy link," in *2015 European Microwave Conference (EuMC)*, pp. 143–146, Paris, France, September 2015.
- [39] G. Monti, L. Corchia, E. D. Benedetto, and L. Tarricone, "Compact resonator on leather for nonradiative inductive power transfer and far-field data links," *Radio Science*, vol. 51, no. 6, pp. 629–637, 2016.
- [40] Y. Amin, J. Hällstedt, S. Prokkola, H. Tenhunen, and L. R. Zheng, "Robust flexible high performance UHF RFID tag antenna," in *2009 11th Electronics Packaging Technology Conference*, pp. 235–239, Singapore, Singapore, December 2009.
- [41] G. Monti, L. Catarinucci, and L. Tarricone, "Broad-band dipole for RFID applications," *Progress in Electromagnetics Research C*, vol. 12, pp. 163–172, 2010.
- [42] Impinj, <http://www.impinj.com>.
- [43] G. Monti and F. Congedo, "UHF rectenna using a bowtie antenna," *Progress in Electromagnetics Research C*, vol. 26, pp. 181–192, 2012.
- [44] G. Monti, L. Corchia, and L. Tarricone, "ISM band rectenna using a ring loaded monopole," *Progress In Electromagnetics Research C*, vol. 33, pp. 1–15, 2012.
- [45] Ettus Research LLC, <http://www.ettus.com>.



Hindawi

Submit your manuscripts at
<https://www.hindawi.com>

